Journal of Porphyrins and Phthalocyanines
J. Porphyrins Phthalocyanines 2019; **23**: 1–9
DOI: 10.1142/S1088424619500196

Published at http://www.worldscinet.com/jpp/

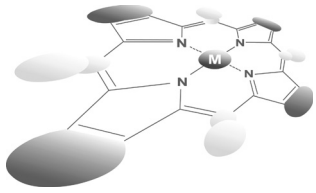

Synthesis, characterization and VOCs adsorption kinetics of diethylstilbestrol-substituted metallophthalocyanines

Esra Kakı*[a], Nurcan Gögsu[a], Ahmet Altındal[b], Bekir Salih[c] and Özer Bekaroğlu*[d]

[a]*Department of Chemistry, Marmara University, 34722, Göztepe, Istanbul, Turkey*
[b]*Department of Physics, Yıldız Technical University, 34220, Istanbul, Turkey*
[c]*Department of Chemistry, Hacettepe University, 06532, Ankara, Turkey*
[d]*Faculty of Pharmacy, Istinye University, Zeytinburnu, 34010, Istanbul, Turkey*

This paper is part of the 2019 Women in Porphyrin Science special issue.

Received 23 November 2018
Accepted 20 January 2019

ABSTRACT: Compound (4,4′-hex-3-ene-3,4-diyl)bis(4,1-phenylene)bis(oxy)diphthalonitrile **3** was synthesized by the reaction of 4-nitrophthalonitrile **1** and diethylstilbestrol **2** in dry DMF in presence of dry K_2CO_3. New mononuclear phthalocyanines **4–6** were obtained from compound **3** by addition of the corresponding metal salts [$Co(OAc)_2 \cdot 4H_2O$, $Zn(OAc)_2 \cdot 2H_2O$ and $Cu(OAc)_2$]. The novel compounds were characterized by elemental analysis and FT-IR, UV-vis, ^{1}H-NMR and MALDI-TOF mass spectroscopy techniques. The effects of four main groups of organic vapors on these novel compounds were studied and discussed. The adsorption kinetics of alkanes (*n*-hexane and *n*-octane), alcohols (methanol and 2-proponal), chlorinated hydrocarbons (dichloromethane and trichloromethane) and amines (diethylamine and triethylamine) on **4–6** were examined using three adsorption kinetic models: the Elovich equation, the pseudo-first-order equations and Ritchie's equation. Results show that the linear regression analysis with respect to the pseudo-second-order rate equations generates a straight line that best fits the data of adsorption of alcohols and chlorinated hydrocarbons on Pc films. On the other hand, the Elovich equation generates a straight line that best fits the data of adsorption of alkanes and amines.

KEYWORDS: phthlocyanine, mononuclear, adsorption kinetics, amines, alkanes.

INTRODUCTION

Phthalocyanines (Pcs) and their metal complexes have been the most studied class of functional organic materials for almost a century. Their conjugated 18π-electron systems have rich electron transfer ability which depend mainly on the metal centers and peripheral or non-peripheral substituents. Their interesting physical, chemical, biological and spectral properties have received increasing attention for applications of Pcs as chemical sensors, optical discs, laser dyes, electrocatalysis, data storage, printing inks and display devices [1], have received increasing attention due to their interesting physical, chemical, biological and spectral properties [1]. In recent years, applications of their complexes have expanded to nonlinear optics [2, 3], liquid crystals [4], gas sensors [5, 6], electrochromism [7, 8], solar cells [9, 10], catalysts [11, 12] and photodynamic therapy (PDT) [13, 14].

Pcs can be prepared by many different routes and at different temperatures. Several formation mechanisms have been postulated depending on starting compounds and in some case on isolated intermediates: it is not necessary that all routes proceed through a common mechanism [1, 15]. In recent years, a new class of Pcs,

*Correspondence to: Esra Kakı, tel.: +90 2163479641, fax.: +90 2163478783, email: ekaki@marmara.edu.tr; Özer Bekaroğlu, tel.: +90 2122852333, fax: +90 2122856386, email: obek@itu.edu.tr.

ball-type, have been synthesized at high temperatures in five minutes using solvent or without solvent. The formation mechanism of these ball-type Pcs can be explained according to the reaction route which proceeds over monomer Pc in some cases first then by further reaction in solvent using excess of metal salts [16a].

Due to strong intermolecular interactions between the macrocycles, most of the peripherally unsubstituted Pcs are hardly soluble in common organic solvents and water. These interactions result in aggregation, which causes difficulties in Pcs separation or identification and minimizes their applications. For this reason, one of the important aim of this investigation is to enhance solubility. When functional groups such as alkyls, alkoxyls, crown ethers and phenoxyls are bound in the peripheral benzene rings of the phthalocyanine structure, solubility of Pcs can improve exceedingly in protic or non-protic solvents [17, 18].

Volatile organic compounds (VOCs) are composed of several gasses: hydrocarbons, solvents and other organic compounds, which usually cause respiratory difficulties and irritation, and which have important effects on low atmospheric cycles, agriculture, medicine and foods. Therefore, the detection of VOCs has become a serious task due to regulations in many countries in the world. Pcs as a group of potential gas sensing materials, have become a natural choice for the detection of VOCs because of their open coordination sites for axial ligation, their large spectral shifts upon ligand binding and their intense coloration [19]. Previous investigations on Pc thin films as gas sensing materials have revealed a high sensitivity to the various organic vapors [5, 20–24]. Unlike the ensign properties and the effect of environmental conditions on the sensing performance of Pc-based sensors, adsorption kinetics of organic vapors on novel metallophthalocyanine thin films have not been widely studied.

Our research has been devoted mostly to face-to-face or ball-type phthalocyanines for the past 15 years and we pioneered research on those compounds, which showed intrinsically more versatile chemical and physical properties. Unfortunately, there papers in the literature on this new class of Pcs are rare. It is well known that depending on the organic groups of the peripheral or non-peripheral positions of phthalocyanines the electronic properties change drastically. Therefore, changing bridged compounds with electron-donating or electron-accepting properties affects the chemical and physical properties of the ball-type phthalocyanines on a large scale. The electronic nature, stereo chemistry of the bridged compounds and the reaction conditions have large effects on the obtained Pcs' structures and properties. For instance, one can obtain direct ball-type, or four-substituted open- or cross adjacent ring-formed Pcs [5, 16a,b], all of which show different chemical and physical properties.

In the present paper, instead of the expected of ball-type Pc, novel mononuclear Pcs have been prepared from [(4,4′-hex-3-ene-3,4-diyl)bis(4,1-phenylene)bis(oxy) diphthalonitrile] (Scheme 1). This study also highlights the adsorption kinetics of four main groups of organic vapors on **4**–**6**. Kinetic models evaluated include the Elovich equation, the first-order rate equation of Lagergren and Ritchie's equation.

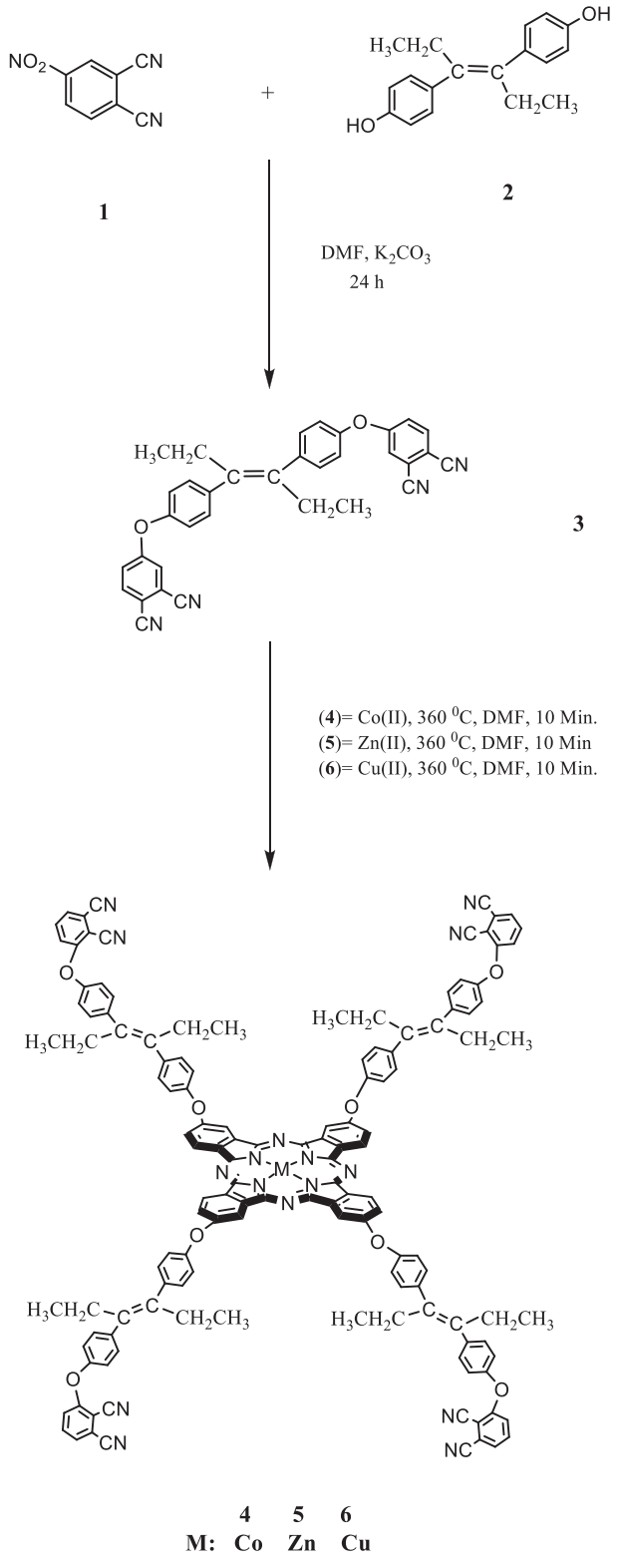

Scheme 1. Synthesis of compounds **3**,**4**,**5** and **6**

EXPERIMENTAL

Materials and instruments

Our starting materials, **1** and **2**, were commercially available. FT-IR spectra were recorded by a Schimadzu FTIR-8300 spectrophotometer. Electronic spectra were recorded by a Schimadzu UV-1601 spectrophotometer. Mass spectra were acquired by a Voyager-DE™ PRO MALDI-TOF mass spectrometer (Applied Biosystems, USA) equipped with a nitrogen UV-Laser operating at 337 nm. Spectra were recorded in positive ion, linear and reflectron modes with an average of 100 shots. Elemental analyses were performed by the Instrumental Analysis Laboratory of TUBITAK-Marmara Research Centre. ^{1}H-NMR spectra were recorded in $CDCl_3$ with a Mercury-VX 400 BB instrument.

Synthesis and characterization

[(4,4′-*hex*-3-*ene*-3,4-*diyl*)*bis*(4,1-*phenylene*)*bis*(*oxy*)-*diphthalonitrile*] 3. 4-Nitrophthalonitrile **1** (0.693 g, 4.0 mmol) and diethylstilbestrol (DES) **2** (0.537 g, 2.0 mmol) were dissolved in 30 mL dry dimethylformamide (DMF). After stirring for 5 min, dry potassium carbonate (K_2CO_3) (1.656 g, 12.0 mmol) was added to this solution with stirring. The reaction mixture was stirred at room temperature for 24 h under a N_2 atmosphere. Then the mixture was poured into cold water (100 mL) and stirred. The formed precipitate was filtered off and washed with water until neutral. The product was obtained by column chromatography with silica gel using chloroform ($CHCl_3$) as eluent. Yield: 0.9886 g (94%). Compound **3** is soluble in $CHCl_3$ dichloromethane (CH_2Cl_2), tetrahydrofuran (THF), DMF, dimethylsulfoxide (DMSO), acetone (C_3H_6O) and acetonitrile (CH_3CN). Mp: 255 °C. Anal. Calc. for $C_{34}H_{24}O_2N_4$: C, 78,44; H, 4,65; N, 10,76%. Found: C, 78,21; H, 4,56; N, 10.93. FT-IR (ν_{max}/cm^{-1}): 827, 953, 1091, 1168, 1248, 1287, 1423, 1482, 1562, 1591, 1677, 2232, 2968. ^{1}H-NMR (400 MHz, $CDCl_3$): δ_H, ppm 0.84 (t, J = 7.4 Hz, 6H), 2.20 (q, J = 7.4 Hz, 4H), 7.10 (d, J = 8.5 Hz, 4H), 7.31 (dd, J = 8.5 and 2.5 Hz, 2H), 7.31 (d, J = 8.5 Hz, 4H), 7.32 (d, 7.33, J = 2 Hz, 2H), 7.75 (d, J = 8.6 Hz, 2H). MS (MALDI-TOF): *m/z* 522 [M+H]$^+$.

[2,10,16,24{*tetrakis*(4,4′-*hex*-3-*ene*-3,4′′-*diyl*)*bis*-(4,1-*phenylene*)*oxydiphthalonitrile*}*phthalocyaninato-cobalt*(*II*)] 4, *zinc*(*II*) 5, *and copper*(*II*) 6. A mixture of compound **3** (2.1×10^{-1} g, 0.40 mmol) and the metal salts [1.0×10^{-1} g, 0.40 mmol $Co(OAc)_2 \cdot 4H_2O$ or 8.8×10^{-2} g, 0.40 mmol $Zn(OAc)_2 \cdot 2H_2O$ or 7.3×10^{-2} g, 0.40 mmol $Cu(OAc)_2$] were transferred into a reaction tube. DMF (0.7 mL) was added to this reaction mixture and the mixture was heated under dry N_2 atmosphere in a sealed glass tube for 10 min at 360 °C. After cooling to room temperature, 4 mL of DMF was also added to the residue to dissolve the product. The reaction mixture was precipitated by adding acetic acid. After filtration, the crude product was washed with acetic acid, water and methanol for 24 h in a Soxhlet apparatus, in order to eliminate the unreacted starting materials. The solid product was purified by column chromatography with silica gel using $CHCl_3$ as eluent. Compound **4** was dark blue, **5** was blue and **6** was blue; all were soluble in DMF, THF and DMSO.

Yield **4**: 31 mg (15%). Mp >350 °C. Anal. Calc. for $C_{136}H_{98}O_8N_{16}Co$: C, 76,21; H, 4,61; N, 10,46%. Found: C, 76,49; H, 4,53; N, 10,67. FT-IR (ν_{max}/cm^{-1}): 751, 854, 954, 1091, 1163, 1228, 1277, 1408, 1472, 1502, 1593, 1738, 1774, 2232, 2871, 2967. UV-vis (DMF): λ_{max}/nm (log ε): 665 (4.529), 606 (4.067), 325 (4.465). MS (MALDI-TOF): *m/z* 2145 [M + H]$^+$.

Yield **5**: 47 mg (23%). Mp >350 °C. Anal. Calc. for $C_{136}H_{98}O_8N_{16}Zn$: C, 75,98; H, 4,59; N, 10,42%. Found: C, 75,63; H, 4,45; N, 10,61. FT-IR (ν_{max}/cm^{-1}): 744, 822, 1043, 1088, 1163, 1227, 1278, 1398, 1475, 1502, 1597, 1714, 1770, 2233, 2870, 2965. UV-vis (DMF): λ_{max}/nm (log ε): 679 (4.542), 610 (3.837), 354 (4.153). ^{1}H-NMR (400 MHz, $CDCl_3$): δ_H, 0.91 (t, J = 7.5, 24H), 2.20–2.30 (m, 16H), 7.05–7.20 (m, 16H), 7.30–7.40 (m, 32H), 7.80 (d, J = 8.5, 8H). MS (MALDI-TOF): *m/z* 2148 [M + H]$^+$.

Yield **6**: 36 mg (18%). Mp >350 °C. Anal. Calc. for $C_{136}H_{98}O_8N_{16}Cu$: C, 76,05; H, 4,60; N, 10,43%. Found: C, 75,82; H, 4,69; N, 10,25. FT-IR (ν_{max}/cm^{-1}): 745, 821, 1090, 1163, 1226, 1277, 1404, 1474, 1501, 1594, 1714, 1770, 2233, 2871, 2964. UV-vis (DMF): λ_{max}/nm (log ε): 677 (4.533), 611 (4.047), 337 (4.310). MS (MALDI-TOF): *m/z* 2149 [M + H]$^+$.

MALDI sample preparation

MALDI matrix 2,5-dihydroxybenzoic acid was prepared in THF-ACN-H_2O (1:3:1, v/v/v) containing 0.2% trifluoroacetic acid at a concentration of 5 mg/mL. The MALDI samples were prepared by mixing sample solutions (0.5 mg/mL in ACN-THF-H_2O mixture (1:3:1, v/v/v) having 0.3% trifluoroacetic acid) with the matrix solution (1:10, v/v) in a 0.5 mL Eppendorf® micro tube. Finally 0.5 µL of this mixture was deposited on the sample plate, dried at room temperature and then analyzed.

VOC vapor sensing measurements

Metallophthalocyanine-based gas sensors were prepared as reported previously [25]. Substrates were 10×10 mm^2 glass slides with photolithographically patterned gold interdigitated electrodes (IDEs); the IDEs contained 10 finger pairs with a channel length of 50 µm and a width of 50 µm. The 120-nm-thick sensor films of MPcs were deposited on IDEs by the spin coating method using a spinner (Speciality Coatings Systems Inc., Model P6700 Series). The elipsometric technique was used to measure the thickness of the Pc film. Because of the good solubility of the compounds, DMF was used as the solvent. Substrate temperature during deposition was held constant at 25 °C to maintain constant film

morphology across all sensors. The sensing properties of the coating material were tested in a cylindrical chamber of Teflon, 8 cm long and 4 cm diameter, through which a gas could be passed. During sensing experiments, the chamber temperature was maintained at 25 °C. Zero grade air was used as the carrier gas, with a constant flow rate of 100 standard cubic centimeter per min (sccm). Analytes were chosen to span a range of organic vapors. These included alcohols (methanol and 2-proponal), amines (diethylamine and triethylamine), chlorinated hydrocarbons (dichloromethane and trichloromethane) and alkanes (*n*-hexane and *n*-octane). The variation of the sensor currents were measured by applying a constant dc bias of 1 V and monitoring the current using a Keithley model 6517A electrometer.

RESULTS AND DISCUSSION

Synthesis and characterization

The substituted diphthalonitrile compound **3** was obtained by reaction between 4-nitrophthalonitrile **1** and diethylstilbestrol **2**. In this reaction, dry K_2CO_3 and dry DMF were used as a base and solvent, respectively. Next, the complexes **4–6** were synthesized by heating **3** with $Co(OAc)_2 \cdot 4H_2O$, $Zn(OAc)_2 \cdot 2H_2O$ or $Cu(OAc)_2$, respectively, under N_2 atmosphere in a sealed tube (Scheme 1).

All the new compounds obtained in this study have been characterized by spectroscopic techniques such as elemental analyses, FT-IR, ^{1}H-NMR, UV-vis and MALDI-TOF mass spectrometry. The spectroscopic data of compounds **3–6** confirmed the proposed structures.

The IR spectra of compounds **3–6** showed CN group peaks at 2232–2233 cm^{-1} as a single peak, Ar-O-Ar peaks at 1250–1280 cm^{-1}, aromatic C=C peaks at 1560–1590 cm^{-1}, C=N peaks at 1715–1737 cm^{-1}, C=C peaks at 1675 cm^{-1} and aliphatic CH peaks at 2870–2960 cm^{-1}.

The UV-vis spectra of the phthalocyanine core is dominated by two intense bands, a Q band in the visible part of the spectrum around 600–700 nm, is attributable to the $\pi \rightarrow \pi^*$ transitions from the highest occupied molecular orbital (HOMO) to the lowest unoccupied molecular orbital (LUMO) of the phthalocyanine ring. The other bands (B) in the UV region at about 300–400 nm were observed due to the transitions from the deeper π levels to the LUMO. Electronic spectra of the studied Pcs (**4–6**) in DMF are given in Fig. 1. The UV-vis spectra of novel mononuclear Pcs (**4–6**) exhibited Q-band absorption of the $\pi \rightarrow \pi^*$ transitions at 610 and 680 nm. The ground-state electronic absorption spectra of **5** and **6** showed monomeric behavior evidenced by a narrow Q band at 675 nm, whereas the Q band of **4** is observed at 666 nm, which is broadened and blue shifted, indicating H aggregation. Aggregation is usually depicted as a co-planar association and is dependent on concentration. In the aggregation state, the electronic structure of complexed Pc rings is perturbed, resulting in alteration of the ground- and excited-state electronic structures [26, 27]. This causes the broadening or split of the absorption bands, especially at high concentrations [28]. The B bands of these Pcs appeared in the UV region at around 325–355 nm and were usually stronger than the Q bands in the case of aggregation [26].

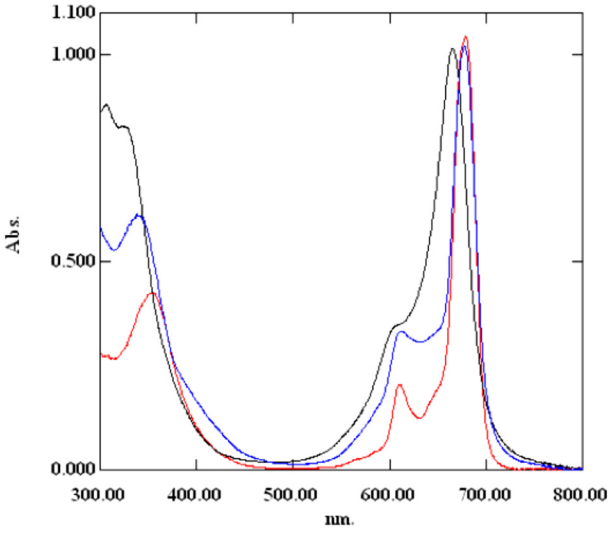

Fig. 1. UV-vis spectra of **4–6** in DMF at 3×10^{-5} M. Absorption spectra of **4** (black), **5** (red) and **6** (blue)

Positive ion and linear mode MALDI-TOF MS spectra of cobalt, zinc and copper complexes were obtained and are given in Fig. 2, respectively. 2,5-dihydroxybenzoic acid MALDI matrix yielded intense protonated molecular ion signals and low fragmentation under the MALDI-TOF MS conditions for these compounds. Positive ion and reflectron mode MALDI-TOF MS spectra for zinc complexes (Fig. 2b) were obtained successfully without any fragmentation. Mass spectra of the cobalt and copper complexes could be obtained only in positive ion and linear modes. To increase the solubility, not only analytes but also the MALDI matrix solution mixture (THF-ACN-H_2O), 1:3:1, v/v/v) were used, and trifuloroacetic acid concentration was increased from 0.1% to 0.3%. Cobalt and copper complexes showed up to 3 water adduct signals showing the water sensitivity of these complexes in the gas phase (Figs 2a and 2c). In the case of cobalt complexes, the main intense fragmentations were because of the dicyanophenyl leaving group. However, the intensities of these fragmentation signals are very low compared to protonated and water adduct signals. From these results, it could be concluded that the metal complexes were synthesized in correct routes in this study as designed.

Sensing properties and adsorption kinetics

In order to investigate the adsorption kinetics of four main groups of organic vapors on thin films of **4–6**,

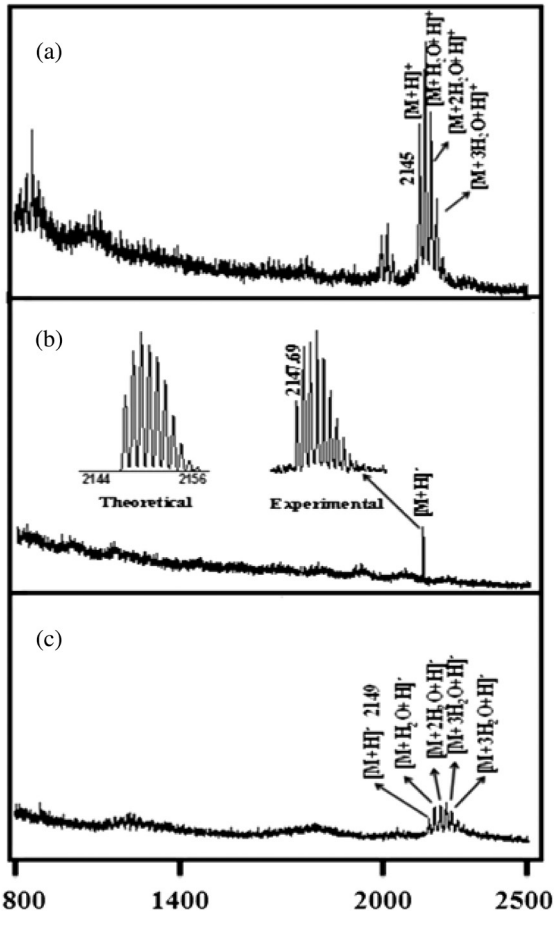

Fig. 2. Positive ion MALDI mass spectra of the complexes were obtained in 2,5-dihydroxybenzoic acid MALDI matrix using nitrogen laser (at 337 nm wavelength) accumulating 100 laser shots. (a) $C_{136}H_{98}CoN_{16}O_8$ in linear mode, (b) $C_{136}H_{98}ZnN_{16}O_8$ in reflectron mode and (c) $C_{136}H_{98}CuN_{16}O_8$ in linear mode

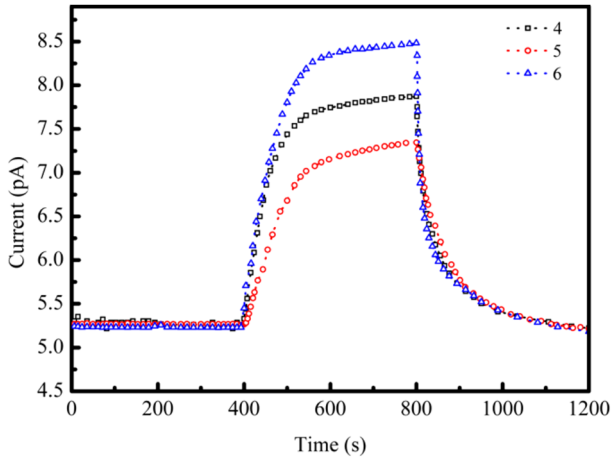

Fig. 3. Effect of 400 ppm dichloromethane vapor on the conductivity of the **4**–**6** coated sensors

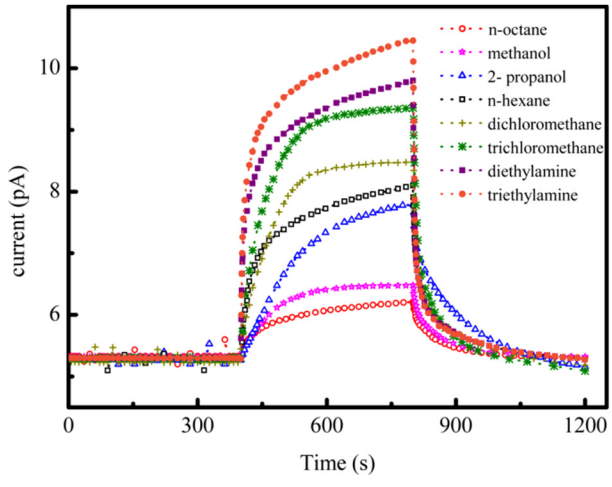

Fig. 4. Response-recovery characteristics of the **6** to the same concentration (400 ppm) of analyte molecules

response-recovery characteristics of the films towards alcohols, amines, chlorinated hydrocarbons and alkanes were carefully examined. As a representative result, the effect of the 400 ppm concentrations of dichloromethane vapor on the conductivity of the **4**–**6**-based sensors is shown in Fig. 3. It is obvious from Fig. 3 that the interactions between the phthalocyanine film and the dichloromethane vapor molecules cause a fast increase of sensor current in the initial doping stage, followed by a drift to the steady-state value.

After several minutes of exposure to dichloromethane vapors, purging with dry air led to an initial fast decrease followed by a slow drift, and the sensor current reached its initial value after the dichloromethane vapors were turned off, proving that the adsorption processes are reversible. Although the origin of the VOC vapor response of a Pc film is not yet fully understood, this effect can be attributed to generating acceptor levels by vapor adsorption. It is believed that adsorption take places at the active adsorption sites on the sensing layer and the magnitude of the sensor response is proportional to the number of the adsorption sites. The adsorption of a vapor molecule at an active adsorption site leads to the creation of an acceptor level near the band edge of the Pc. When the number of trapped electrons reach a sufficient value, the Fermi level shifts toward the valence band [29]. This shift in the Fermi level causes a reduction in the speed of the trapping process and the rate of increase in the current slows down. The exposure of the sensor to a reference gas (dry air in our case) leads to the desorption of the adsorbed vapor molecules from the surface of the active sensing layer, decreasing the acceptor concentration and thus the sensor current. The same type of response–recovery characteristics were also obtained for other organic vapors investigated. Figure 4 shows the room temperature response-recovery characteristics of the **6** coated sensors to the four main groups of analytes.

As one of the most important parameters of gas sensors, sensitivity (S) has been attracting more and more attention and much effort has been made to enhance the

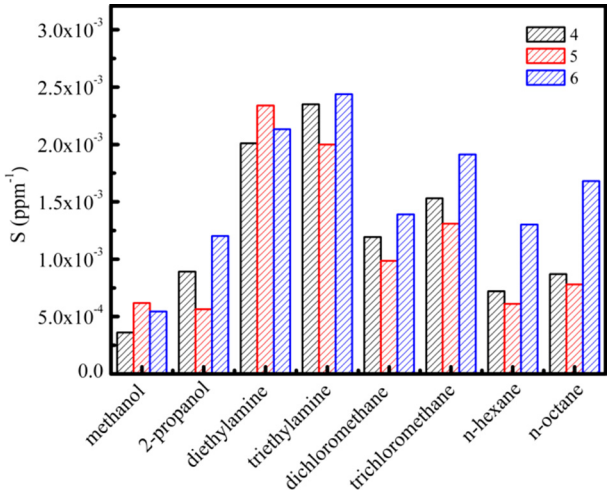

Fig. 5. Sensitivity of the sensors to four main groups of organic vapors

sensitivity of gas sensors. Usually, sensitivity can be defined as (Equation 1):

$$S = \frac{1}{C_i}\left(\frac{\Delta I}{I_0}\right) \quad (1)$$

where ΔI is the changes in current at an organic vapor concentration of C_i, I_0 stands for the current of the device in the reference gas. Figure 5 shows the sensitivity of the sensors to the four main groups of analyte molecules. Maximum sensitivity for the lower and upper limit of analyte concentrations were obtained for amines. Apparently, the sensor with **6** showed maximum sensitivity for all analytes investigated. It was found that the general trend for the order of the sensor sensitivity, observed for the investigated compounds, is S (**6**) > S (**4**) > S (**5**), except for methanol and diethylamine vapors.

It is well documented that the sensing mechanism of VOC vapors by phthalocyanines is not well known. More recent studies indicated that many elementary physicochemical processes should be taken into account to interperet the VOC vapor adsorption onto the phthalocyanine thin film surface. For a particular gas, the intensity and kinetics of the interactions between the phthalocyanine films and the gas molecules are related to the nature of the phthalocyanine compound used as the sensitive material, the charge transport process, the relative orientation and the separation of adjacent molecules. According to Spadavecchia *et al.* [30] the delocalized π-electron system, the presence of heteroatoms and the central metal ion are important features in the organic vapor/MPc interaction mechanism. It is the current opinion that the central metal ion together with the peripheral substituents acts as two different sites of interaction with the analyte molecules. A primary interaction involves the Pc metal and the heteroatoms on the analyte molecule, while a secondary interaction is determined by the peripheral substituents. It is also well established that central metal ions have many influences on the HOMO, LUMO and energy level structures of the complexes, sequentially do the gas sensitivity. It was reported by Bohrer *et al*. [31] and Park *et al*. [32] that the detection of analyte molecules by phthalocyanines is governed primarily by coordination to the metal center. The interaction between the analyte and the metallophthalocyanine surface produces a modulation in the electronic levels of phthalocyanine available for π–π* transitions. As results, a doping effect due to the adsorbed analytes onto the phthalocyanine film is basically the cause of the changes in the conductivity of the sensing layer. These results demonstrate that the organic vapor sensing properties of the [2,10,16,24{tetrakis(4,4′-hex-3-ene-3,4″-diyl)bis(4,1 phenylene)oxydiphthalonitrile} phthalocyaninatocobalt (II)], zinc(II), and copper (II) phthalocyanines are determined by the central metal ion. This findings is consistent with previous observations [33] that observed sensitivities of copper phthalocyanine and nickel phthalocyanine films are different in spite of their similar bond numbers, indicating the significant role of the central metal ion in interaction mechanisms.

Comparisons of kinetic models

Many attempts have been made to formulate a general expression describing the kinetics of sorption on solid surfaces for gas-solid phase sorption systems. However, little has appeared in the literature comparing these different models for gas adsorption on solids. In order to investigate the adsorption mechanism of the four groups of organic vapors onto compounds **4**–**6**, the experimental data were modelled using the first-order rate equation of Lagergren [34], the Elovich model [35] and Ritchie's equation [36], and an attempt has been made to compare them in this work. The conformity between the experimental data and the model predicted values was expressed by the correlation coefficients (R^2).

Elovich model

In reactions involving adsorption of gases on a solid surface, the rate decreases with time due to an increase in surface coverage. The Elovich equation was developed to describe the kinetics of such type of activated sorption of a gas onto solids [37]. The equation defining the Elovich model is based on a kinetic principle assuming that the adsorption sites increase exponentially with adsorption, which implies a multilayer adsorption. This model has been applied satisfactorily to some chemisorption data and the equation is often valid for systems in which the adsorbing surface is heterogeneous. It is expressed by the relation (Equation 2):

$$\frac{dS}{dt} = ae^{-\alpha S} \quad (2)$$

where S is the sorption capacity at time t, a is the initial sorption rate and α is the desorption constant during any one experiment. In the Elovich equation, constant a is regarded as the initial adsorption rate because dS/dt approaches a when S approaches 0 and it depends on the activation energy. Constant α is related to a measure of the extent to which the surface has been screened by the potential barrier for successive adsorption. Assuming that $S = 0$ at $t = 0$; $S = S$ at $t = t$, integrating Equation 2 with these conditions gives Equation 3:

$$S = \frac{1}{\alpha} \ln[a\alpha t + 1] \tag{3}$$

By assuming that $a\alpha t >> 1$, as suggested by Chien and Clayton [38] , Equation 3 becomes Equation 4:

$$S = \frac{1}{\alpha} \ln(t) + \frac{1}{\alpha} \ln(a\alpha) \tag{4}$$

By assuming that the change in the current is proportional to the change in surface coverage [39], a plot of ΔI *vs*. ln (t) should be a straight line. Figure 6 demonstrates the fitting of the adsorption kinetic data and Elovich equation. The validity of the kinetic models is tested by the magnitude of the regression coefficient R^2. It is important to note that for the Elovich equation, the correlation coefficient is always less than 0.98 for methanol, 2-propanol, dichloromethane and trichloromethane which is indicative of a bad correlation. This confirms that the Elovich model is not appropriate to predict the adsorption kinetics methanol, 2-propanol, dichloromethane and trichloromethane onto compound **6** for the entire adsorption period. On the other hand, the Elovich equation provides the best correlation for *n*-octane, *n*-hexane, diethylamine and triethylamine sorption processes and also fits the experimental data well with the regression coefficient larger than 0.99.

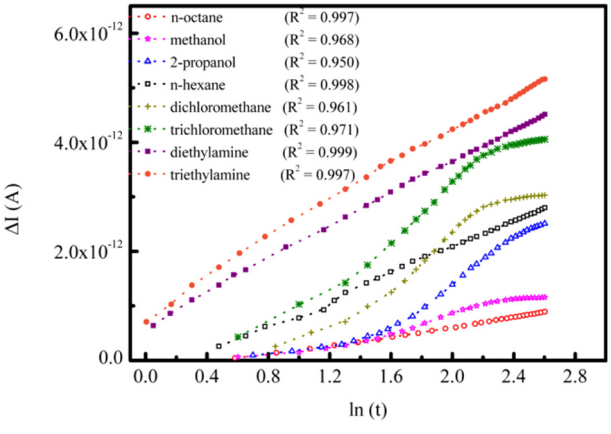

Fig. 6. Elovich plots for the adsorption of analytes on **6**

Ritchie's equation

Ritchie's [36] equation is also widely used in the adsorption of gas particles onto solid systems. Assuming that the rate of adsorption depends solely on the fraction of sites which are unoccupied at time t, Ritchie's second order equation based on adsorption equilibrium capacity is expressed in the form Equation 5:

$$\frac{d\theta}{dt} = b(1-\theta)^m \tag{5}$$

where θ is the fraction of surface sites which are occupied by adsorbed VOC vapor, m is the number of surface sites occupied by each molecule of the adsorbed VOC vapor, and b is the rate constant. By applying the boundary conditions: $\theta = 0$ at $t = 0$ and $\theta = q_t/q_e$ at $t = t$, the integrated form of Equation 5 becomes Equations 6 and 7:

$$\frac{1}{(1-\theta)^{m-1}} = (m-1)\, bt + 1 \quad \text{for } m \neq 1 \tag{6}$$

$$\theta = 1 - e^{-bt} \quad \text{for } m = 1 \tag{7}$$

It is assumed that no site is occupied at $t = 0$. When introducing the amount of adsorption q_t at time t, then Equation 7 becomes Equation 8:

$$\frac{q_e^{m-1}}{(q_e - q_t)^{m-1}} = (m-1)\, bt + 1 \tag{8}$$

If the VOC vapor adsorption is considered to be a second-order reaction, then Equation 8 can be rewritten as Equation 9:

$$\frac{1}{q_t} = \frac{1}{bq_e t} + \frac{1}{q_e} \tag{9}$$

According to Equation 9, if the adsorption processes follows Ritchie's equation, a plot of $(1/q_t)$ *vs*. $1/t$ should be a straight line. Figure 7 shows $(1/q_t)$ *vs*. $1/t$ plots for all analyte vapors at room temperature. As can be seen from Fig. 7, the correlation coefficients, R^2, are in the range of 0.537–0.860 for all analytes investigated, which is indicative of a bad correlation. This confirms that Ritchie's equation is not appropriate to use as a model to predict the adsorption kinetics of these analytes' vapor onto compound **6**.

The pseudo-first-order model

Lagergren [34] suggested a model for the sorption system based on the adsorption capacity. This model assumes that the rate of occupation of adsorption sites is directly proportional to the number of unoccupied sites. When adsorption is preceded by diffusion through a boundary, the kinetics follows the pseudo-first-order rate

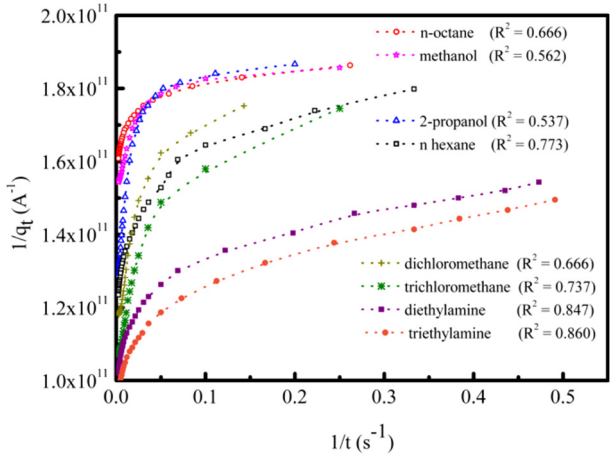

Fig. 7. Plots of Ritchie's equation for sorption of the indicated vapors onto the compound **6**

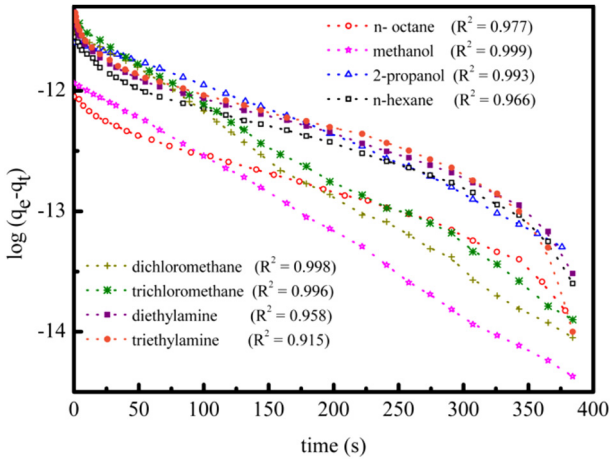

Fig. 8. Pseudo-first-order sorption kinetics of analytes onto the compound **6**

equation of Lagergren and can be represented as follows (Equation 10):

$$\frac{dq_t}{dt} = k_{ads}(q_e - q_t) \tag{10}$$

where q_e and q_t are the amounts of analyte vapor adsorbed at equilibrium and at any time t, respectively. k_{ads} is the first-order adsorption rate constant. Integrating Equation 10 for boundary conditions at $t = 0$ to $t = t$ and $q_t = 0$ to $q_t = q_t$, results in the following (Equation 11):

$$\ln\left(\left(\frac{q_e}{q_e - q_t}\right) = k_{ads}t\right) \tag{11}$$

which may be rearranged to (Equation 12):

$$\log(q_e - q_t) = \log q_e - \frac{k_{ads}}{2.303}t \tag{12}$$

To quantify the applicability of the first-order model, the correlation coefficient was calculated from the response-recovery characteristics of the sensors. Figure 8 shows a plot of the linearized form of the first-order model for all analytes investigated. A considerable deviation from the theoretical model is clear for *n*-octane, *n*-hexane, diethylamine and triethylamine vapors, the pseudo-first-order equations do not give a good fit to the experimental data for the adsorption of these organic vapors on **6**. The low correlation coefficients for the first-order kinetic model obtained for these organic vapors suggests that this adsorption system is not a pseudo first-order reaction.

CONCLUSION

The novel substituted diphthalonitrile compound **3** and its mononuclear Pcs (**4–6**) have been synthesized for the first time in this study. The complexes were characterized by elemental analysis, UV-vis, IR and MALDI-TOF mass spectroscopies. Spin-coated films of compounds **4–6** were used to sense four main groups of organic vapors based on the changes in the electrical conductivity. It was found that the interaction of the organic vapors with the spin-coated films led to significant changes in electrical conductivity. The response and sensitivity are dependent on the central metallic ion, which shows the possibility of changing the sensor sensitivity with minor modifications of the synthesis process. Maximum sensitivity was obtained with 6 coated sensors for all organic vapors investigated. A comparative study of the applicability of kinetic models of Elovich equation, Ritchie's equation and first-order model to describe the experimental adsorption data of the analyte vapors on Pc compounds has been carried out. Comparing the regression coefficients, R^2, shows that adsorption kinetics depend on the nature of the reactant vapor molecules but are independent from the metal ion of the sensing film. The results reveal that the adsorption of alkanes and amines onto Pcs can be successfully described by the Elovich equation. On the other hand, it was found that the adsorption of alcohols and chlorinated hydrocarbons on Pcs follow the first-order rate equation of Lagergren.

Acknowledgments

We thank the Turkish Academy of Sciences TUBA and Marmara University and the Commission of Scientific Research Projects (Project No: Science-C-YLP-121114-0360) for their support. This study was also supported by the Yıldız Technical University Commission of Scientific Research Projects under Grant No. 2014-01-01-YL01 and 2014-01-01-KAP01.

REFERENCES

1. (a) Leznoff CC and Lever ABP. *Phthalocyanines Properties and Applications,* Vol. 1, 1989 and Vol. 3,

VCH: New York, 1993, (b) Moser FH and Thomas CR. *Phthalocyanine Compounds,* Reinhold: New York, 1963, (c) Kadish KM, Smith KM and Guilard R. *The Porphyrin Handbook,* Academic Press: Amsterdam, 2003.
2. De la Torre G, Vazquez P and Agulla-Lopez F and Torres T. *Chemical Reviews,* 2004; **104**: 3723–3750.
3. Zhang W, He C, Zhang L, Jiang L, Yuan Y and Wang B. 2018; **22**: 863–867.
4. Ishikawa K, Watarai A, Yasutake M and Ohta K. *J. Porphyrins Phthalocyanines.* 2018; **22**: 693–715.
5. Kakı E, Altındal A, Salih B and Bekaroğlu Ö. *Dalton Trans.* 2015; **44**: 8293–8299.
6. Pişkin M, Can N, Odabaş Z and Altındal A. *J. Porphyrins Phthalocyanines.* 2018; **22**: 189–197.
7. Abdurrahmanoğlu Ş, Özkaya AR, Bulut M and Bekaroğlu Ö. *Dalton Trans.* 2004: 4022–4029.
8. Orman EB, Odaba Z and Özkaya AR. *Journal of The Electrochemical Society.* 2018; **165**: H530–H548.
9. Urbani M, Ragoussi ME, Nazeeruddin MK and Torres T. *Coordination Chemistry Reviews.* 2019; **381**: 1–64.
10. Fischer MKR, Lopez-Duarte I, Wienk MM, Martinez-Diaz MV, Janssen RAJ, Bauerle P and Torres T. *J. Am. Chem. Soc.* 2009; **131**: 8669–8676.
11. Yılmaz F, Özer M, Kani İ and Bekaroğlu Ö. *Catal. Lett.* 2009; **130**: 642–647.
12. Türker Acar E, Akkızlar Tabakoğlu T, Atilla D, Yüksel F and Atun Gülten. *Polyhedron.* 2018; **152**: 114–124.
13. Chen J, Fang Y, Liu H, Chen N, Chen S and Xue J. *J. Porphyrins Phthalocyanines.* 2018; **22**: 807–813.
14. Almeida-Marrero V, Van de Winckel E, Anaya-Plaza E, Torres T and De la Escosura A. *Chem. Soc. Rev.* 2018; **47**: 7369–7400.
15. Elvidge JA and Barot NR. *In the Chemistry of Double Bonded Functional Groups*, Part 2, 5. Patai, ed. Wiley: London, 1977: 1167.
16. (a) Ağırtaş MS, Altındal A, Salih B, Saydam S and Bekaroğlu Ö. *Dalton Trans.* 2011; **40**: 3315–3324, (b) Elmalı D, Altındal A, Özkaya AR, Salih B and Bekaroğlu Ö. *Dalton Trans.* 2011; **40**: 651–660.
17. Banfi S, Caruso E, Buccafurni L, Ravizza R, Gariboldi M and Monti E. *J. Organomet. Chem.* 2007; **692**: 1269–1276.
18. Koçak M, Cihan A, Okur Aİ, Gül A and Bekaroğlu Ö. *Dyes Pigm.* 2000; **45**: 9–14.
19. Mızrak B, Altındal A and Abdurrahmanoğlu Ş. *Prog. Org. Coat.* 2017; **109**: 92–96.
20. Mukhopadhyay S, Hogarth CA, Thorpe SC and Cook MJ. *J. Mater. Sci.: Mater. Electron*. 1994; **5**: 321–323.
21. Spadavecchia J, Ciccarella G, Valli L and Rella R. *Sens. Actuators, B*. 2006; **113**: 516–525.
22. Fietzek C, Bodenhoefer K, Hees M, Haisch P, Hanack M and Göpel W. *Sens. Actuators, B*. 2000; **65**: 85–87.
23. Rodriguez-Mendez ML, Souto J, De Saja R, Martinez J and De Saja JA, *Sens. Actuators, B*. 1999; **58**: 544–551.
24. Kakı E, Özkaya AR, Altındal A, Salih B and Bekaroğlu Ö. *Sens. Actuators, B*. 2013; **188**: 1033–1042.
25. Odabaş Z, Altındal A, Özkaya AR, Salih B and Bekaroğlu Ö. *Sens. Actuators, B*. 2010; **145**: 355–366.
26. (a) Kobayashi N and Lever ABP. *J. Am. Chem. Soc.* 1987; **109**: 7433–7441, (b) Kobayashi N, Hiyashi Y and Osa T. *J. Chem. Soc.*; *Chem. Commun.* 1994: 1785–1786, (c) Dominguez DD, Snow AW, Shirk JS and Pong RGS. *J. Porphyrins Phthalocyanines* 2001; **5**: 582–592.
27. Mishra A, Behera RK, Behera PK, Mishra BK and Behera GB. *Chem. Rev.* 2000; **100**: 1973–2011.
28. Yaho H, Domoto K, Isohashi T and Kimurra K. *Langmuir* 2005; **21**: 1067–1073.
29. Grządziel L, Żak J and Szuber J. *Thin Solid Films* 2003; **436**: 70.
30. Spadavecchia J, Ciccarella G and Rella R. *Sens. Actuators, B*. 2005; **106**: 212–220.
31. Bohrer FI, Sharoni A, Colesniuc C, Park J, Schuller IK, Kummel AC and Trogler WC. *J. Am. Chem. Soc.* 2007; **129**: 5640–5646.
32. Park J, Yang RD, Colesniuc CN, Sharoni A, Jin S, Schuller IK, Trogler WC and Kummel AC. *Appl. Phys. Lett.* 2008; **92**: 193311–193313.
33. Ridhi R, Singh S, Saini GSS and Tripathi SK. *J. Phys. Chem. Solids*. 2018; **115**: 119–126.
34. Lagergren S. *K. Sven. Vetenskapsakad. Handl.* 1898; **24**: 1–39.
35. Tongpool and Yoriya S. *Thin Solid Films* 2005; **477**: 148–152.
36. Ritchie AG. *J. Chem. Soc. Faraday Trans.*1. 1977; **73**: 1650–1653.
37. Low MJD. *Chem. Rev.* 1960; **60**: 267–312.
38. Chien SH and Clayton WR. *Soil Sci. Soc. Am. J.* 1980; **44**: 265–268.
39. Gardner JW, Iskandarani MZ and Bott B. *Sens. Actuators, B.* 1992; **9**: 133–142.